Characteristics of Partial Discharge Induced by Continuous X-ray Exposure of Void Defects in Insulator

Ji-Yong Shin and **Eun-Hee Kim**
Department of Energy Systems Engineering, Seoul National University
1 Gwanak-ro, Gwanak-gu, Seoul 08826, South Korea

Sung-Wook Kim, Hyang-Eun Jo and **Jae-Ryong Jung**
Power Asset Management Team, Power & Industrial Systems R&D Center, Hyosung Corporation
171 Yeondeok-ro, Seongsan-gu, Changwon 51529, South Korea

ABSTRACT

Partial discharge (PD) diagnosis is a part of a routine testing of solid insulating materials to detect void defects. However, the conventional diagnosis is prone to inception delays due to lack of initiatory electron production, especially inside small voids. In this study, we employed continuous irradiation of X-rays to induce and sustain discharge inside the voids. The PD characteristics of void samples under different exposure rates of X-rays were observed. Compared with the conventional diagnosis, this continuous X-ray-induced partial discharge diagnosis enhanced the detection efficiency by eliminating the inception delays and reducing the discharge inception voltage. We focused on the changes in PD characteristics due to varying X-ray exposure rates. As the exposure rates were increased, the number of PD signals per minute increased while the average pulse height of PD signals decreased. Continuous X-ray exposure at rates between 0.5 and 294 mR/s successfully eliminated the inception delays even when the voids were as small as 1.63 mm in diameter of equivalent spherical volume.

Index Terms — **partial discharge, gas insulated switchgear, X-ray exposure, epoxy resin insulator**

1 INTRODUCTION

PHYSICAL defects such as air voids can occur during the manufacture of insulating materials. Small air voids inside the spacers of gas-insulated switchgear (GIS) can make the installations vulnerable to dielectric breakdowns. Enhanced manufacturing process significantly reduces the occurrence of void defects inside the insulating materials [1]. In addition, insulating materials are examined for possible void defects in two separate procedures. Void defects with diameters larger than 7 mm can be manually sorted out via X-ray imaging, and smaller voids are detected using partial discharge (PD) diagnosis based on IEC 60270 standard.

The conventional PD diagnosis proceeds by applying test voltage to the insulating material and detecting the discharge signals that would be triggered in the embedded void defects [2,3]. The discharge inception is often delayed due to the lack of electrons initiating avalanche. In consideration that the inception delay is inversely proportional to the void volumes [4,5], smaller voids make the diagnostics more challenging. When void defects are smaller than 2 mm in diameter, for example, inception delays can be longer than the testing interval of 1 min [6]. Such inception delay can be critical to quality assurance.

Inception delays can be avoided if initiatory electrons are produced inside the void at the time of voltage application. Previous studies pointed out volume generation and surface emission as two main mechanisms of electron generation in the voids [4, 5, 7]. X-ray irradiation can facilitate both photoionization of gas molecules (volume generation) and electron detrapping from void surfaces (surface emission) [8].

Several studies incorporated X-ray irradiation in the conventional PD diagnosis. Since the 1980s, the continuous X-ray-induced partial discharge (XIPD) has been investigated [9-13]. The feasibility of the XIPD technique in void detection was tested at exposure rates as high as 22 mR/s [9,10]. The XIPD technique results in the disappearance of inception delays and the reduction of discharge inception voltage (DIV). Continuous X-ray irradiation also changes the statistical characteristics of PD, such as increasing the number of PD signals and decreasing PD pulse heights [13]. The assembled XIPD system demonstrates significant improvement in the efficiency and precision of quality control. A relatively lower exposure rate of 0.5 mR/s has been suggested for the testing of GIS spacers because high exposure rate might inhibit the discharge activity [11-13], but the range of high exposure rate

Manuscript received on 14 January 2019, in final form 1 May 2019, accepted 2 May 2019. Corresponding author: E.-H. Kim.

DOI: 10.1109/TDEI.2019.008052

has not been specified. Given that the exposure rates were not directly measured, the suggested irradiation level can have significant uncertainty.

A PD diagnosis was also conducted by employing a pulsed X-ray beam [14-16]. This pulsed X-ray-induced partial discharge (PXIPD) technique eliminates inception delays and thus facilitates void detection [15]. Unlike XIPD, PXIPD results in the same discharge characteristics as the conventional PD [15, 16]. The DIVs are in good agreement with the theoretical inception criteria [16]. It was presumed that the pulsed beam produces the initiatory electrons for the first PD only and does not affect the subsequent PD activities [16].

This research is the first part of a project, focused on enhancing the routine PD testing by eliminating inception delays. Under a given X-ray irradiation, the exposure rate varies depending on the location of a void because of the varying degrees of source beam attenuation. A suitable range of exposure rates delivered to the voids should be determined first because the discharge characteristics vary according to the X-ray exposure rates in voids. However, few studies about XIPD or PXIPD have mentioned the effects of X-ray exposure rates on PD characteristics. In the present study, we investigated the PD characteristics in the XIPD test by focusing on the number of PD signals per minute and the average height of PD signals at different X-ray exposure rates to provide a quantitative basis for the XIPD technique.

2 MATERIALS AND METHODS

2.1 VOID SAMPLES

Void samples were fabricated by injecting air into epoxy-alumina bodies using a syringe (Figure 1a). The epoxy-alumina bodies were shaped into thin cylinders. The voids were irradiated in the radial direction of cylindrical bodies with the brass electrodes attached in the axial direction (Figure 1b). The dimensions of the test void samples are listed in Table 1. Samples D5H5 and D5H4 represent relatively larger voids that have shorter inception delays but still require PD testing to be detected. They were employed to study the exposure rate effects of XIPD, which include the number of PD signals per minute, PD pulse heights, and changes in phase-resolved partial discharge (PRPD) pattern. The critical and detectable void defects in GIS are 3-4 and 2-3 mm in diameter, respectively [1]. D1H1 sample represents smaller void defects that can frequently pass through conventional PD tests undetected.

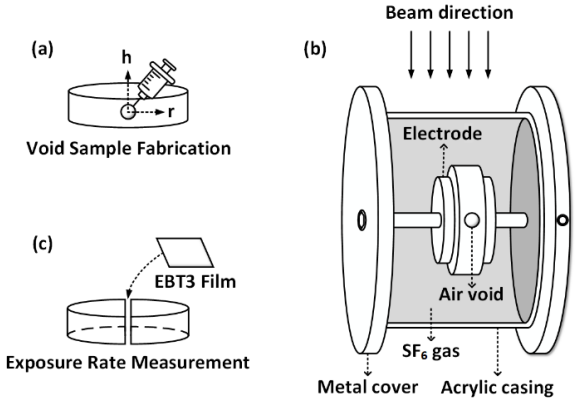

Figure 1. Setups for (a) fabrication of test void samples in cylindrical epoxy-alumina bodies, (b) XIPD diagnosis with voids under exposure, and (c) measurement of exposure rates in voids.

Table 1. Dimensions of voids embedded in epoxy-alumina bodies.

Sample ID	Spheroidal Air Void		Cylindrical Epoxy-alumina Body
	Diameter (mm)	Height (mm)	Height (mm)
D5H5	5.50	5.38	9.80
D5H4	5.61	4.57	8.60
D1H1	1.61	1.72	6.00

2.2 LAYOUT OF EXPERIMENT

Each void sample was positioned inside a PD test cell, which encapsulates a void sample, a pair of brass electrodes, and SF_6 gas inside an acrylic casing (Figure 1b). The test cell was connected to a high voltage source (HPA-505FC3, High Voltage Inc., USA) and a coupling capacitor (MCC-210L, Omicron, Germany) as shown in Figure 2. PD measurement proceeded following the IEC 60270 standard. The control panels were positioned outside the X-ray room to ensure the safety of research staff.

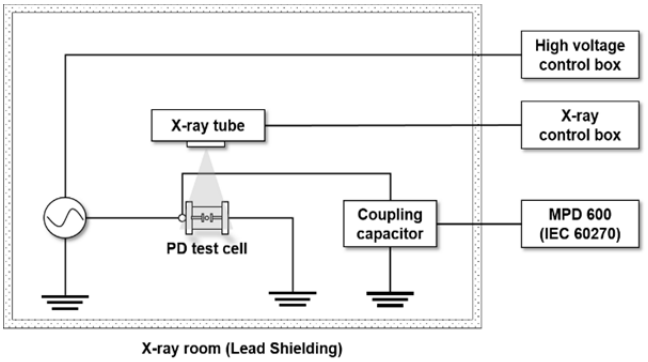

Figure 2. Layout of the experimental setting.

The circuit in Figure 2 was calibrated without high voltage using CAL 542 calibrator and MPD/MI software (Omicron, Germany). The noise level was maintained below 20 pC at voltages under 20 kV (Figure 3a). At the applied voltage of 15 kV, no discharge without X-ray exposure was observed, whereas the smallest PD pulse height from void sample D1H1 was approximately 150 pC under X-ray exposure (Figure 3b).

2.3 X-RAY EXPOSURE RATE MEASUREMENT

X-ray beam exposure was made in the HardX-SNU facility installed with an YXLON X-ray tube (Model 450-D08, Germany) [17]. The tube was operated at 150 kVp to generate bremsstrahlung X-rays in a tungsten target.

The chance of producing initiatory electrons in voids increases with exposure rate in voids. Previous studies calculated the exposure rates of continuous or pulsed X-rays

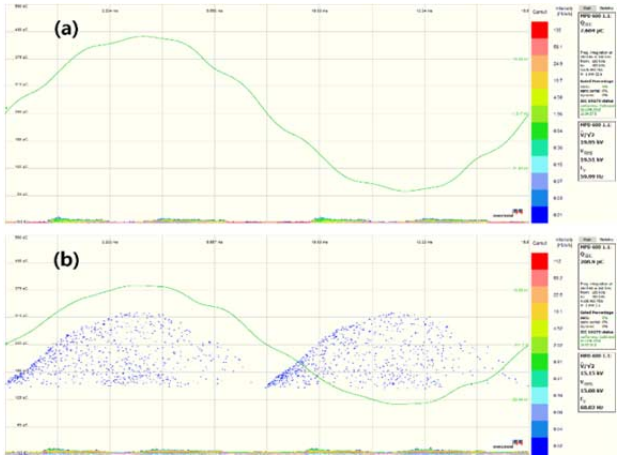

Figure 3. Screenshots from the Omicron software work: (a) noise level of the circuit at 20 kV, and (b) PD signal from the D1H1 void sample at 15 kV along with the noise floor at the bottom.

delivered to the voids by adopting attenuation coefficients of the structure materials containing voids, but such approximation can result in considerable uncertainties. Instead, we measured the exposure rate in voids using Gafchromic EBT3 films (International Specialty Products, USA) [17-18]. A slice of the film was placed between a pair of semi-cylindrical epoxy-alumina composite (Figure 1c) and was positioned the same way as the experimental setup. Exposure rate was modulated by adding 3.6 or 6.0 mm-thick copper filters at the beam exit of the X-ray tube. Exposure rate was estimated by the change in film optical density after X-ray exposure [17]. We managed the exposures delivered to the voids at 0.5-4.0 mR/s by 0.5 mR/s of interval and at 20 and 294 mR/s.

2.4 XIPD EXPERIMENT

The initial test voltage was set at a level low enough to prevent triggering PD in void samples. The first X-ray exposure of a void sample was made 1 min after reaching the initial test voltage. X-ray exposure of the void sample proceeded after every 1 kV of voltage increase up to 20 kV (Figure 4). The X-ray exposure lasted for 1 min at every voltage level. The whole process was repeated for each void sample and at different exposure rates.

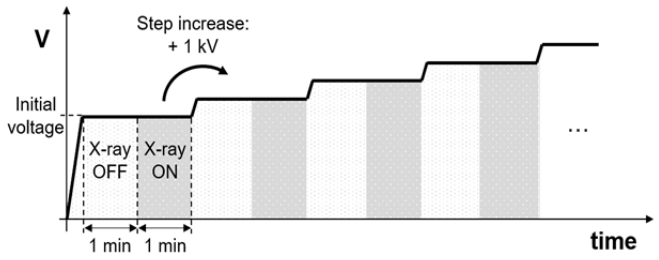

Figure 4. Control of the voltage applied to the electrode for the sequential X-ray exposures of a void sample.

For every PD inception, the number of PD signals per minute, the average pulse height of PD signals, and PRPD pattern were recorded using MPD 600 (Omicron, Germany). At each experimental setup, multiple (3-5) data sets were obtained. Every sequential test with the same void sample proceeded at more than 4 h of delay to avoid the influence of previous PD activity.

3 RESULTS

Figure 5 presents XIPD inceptions in void samples of two sizes from X-ray exposure at different exposure rates as the applied voltage was increased by 1 kV. The Y-axis on the right indicates the applied electric field, which was calculated by dividing the voltage applied to the epoxy alumina body by the thickness of the body. PD occurred under electric fields over the threshold that was specific to the size of void sample: 2.5 kV/mm in D1H1 versus 2.0 kV/mm in D5H4 at an exposure rate of 2.5 mR/s (Figures 5a vs. 5b). A smaller void sample requires a higher threshold for PD, which complies with the streamer criterion for inception field [4-5]. When the exposure rate was leveled up to 294 mR/s, the threshold for PD inception did not change (2.5 kV/mm), whereas the average PD pulse height was reduced from 2020 pC to 1550 pC (Figures 5b vs. 5c).

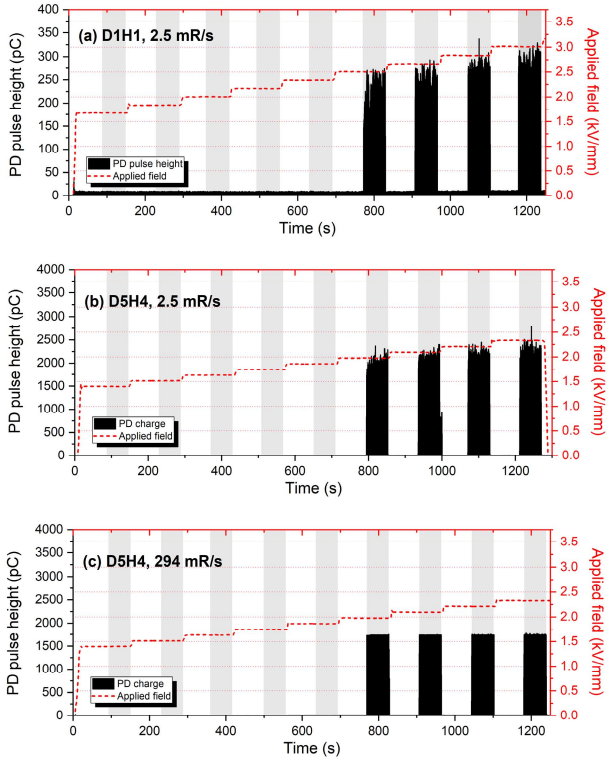

Figure 5. Examples of PD inception in void samples of different sizes (a vs. b) and at different X-ray exposure rates (b vs. c), observed by increasing the applied voltage by 1 kV. (Shaded areas for X-rays on)

As shown in Figure 6, with large void samples (D5H5 and D5H4), the number of PD signals per minute increased rapidly with increasing exposure rate up to 3 mR/s and reached a saturation point of 7000 PDs per minute. With the small void sample (D1H1), on the other hand, the number of PD signals increased relatively slowly to the saturation value with increasing exposure rate up to 294 mR/s.

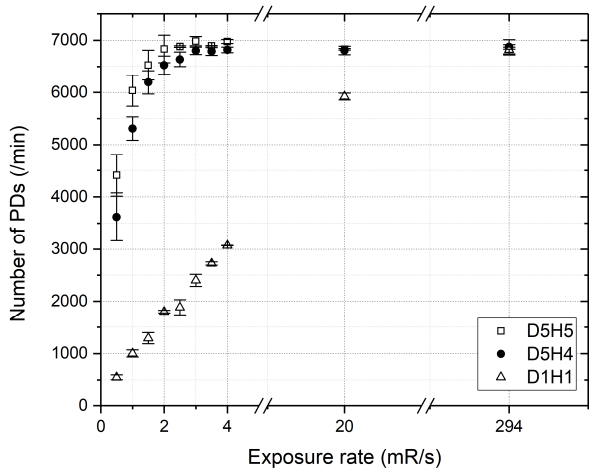

Figure 6. Number of PD signals per minute with void samples of different sizes under varying X-ray exposure rates. The error bars indicate the standard errors.

When electrons are abundantly available inside the void, the number of PD signals per AC half cycle (N_{HW}) saturates to the value determined by the electric field inside the void and the inception field [19]. Our observation implies that the large void samples reach the saturation level of $N_{HW} \approx 0.97$ when the exposure rate is 3 mR/s. Under the same X-ray exposure, the number of electrons generated inside a void is proportional to the void's volume. Thus, sample D1H1 can reach the comparable degree of electron abundancy when the exposure rate is leveled up to approximately 100 mR/s and over. To confirm that the volumetric electron generation rate determines a frequency of PD occurrence, additional experiments using small void samples under the exposure rates between 20 and 294 mR/s should be performed.

Figure 7 depicts that the average PD pulse heights in the void samples reached their maximum values between 1 and 4 mR/s and continuously decreased as the exposure rate was further increased. The reduction of PD pulse heights can be explained in terms of X-ray effect on statistical time lags, which is further elaborated in the following section.

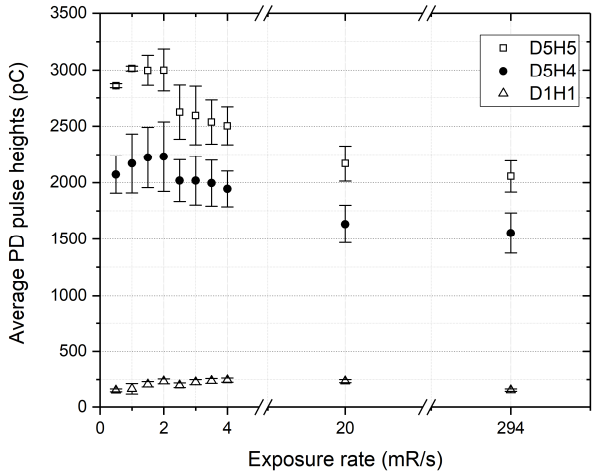

Figure 7. PD pulse heights in the void samples of different sizes under varying X-ray exposure rates.

Overall, the small void samples responded with PD signals that were less in number and smaller in charge as compared with the large void samples. In addition, changes in PD characteristics, such as the increased number of PD signals and reduced PD pulse heights, were observed in all void samples. Increasing X-ray exposure rates up to 294 mR/s did not result in PD inhibition as reported in several studies [11–14].

4 DISCUSSION

4.1 X-RAY EFFECT ON STATISTICAL TIME LAG

Our observations (Figures 5-7) implied the following: (1) PD occurs at applied voltages exceeding DIV under X-ray exposure; (2) the number of PD signals increases up to saturation point with X-ray exposure rates; and (3) the average PD pulse heights are reduced at high exposure rates. Here, we discuss these changes in PD characteristics due to X-ray exposure from the statistical time lag point of view.

Figure 8 depicts a scheme for judging PD inception in a void sample based on the electric field inside the void and the chance of generating initiatory electrons, which was simplified from an earlier work [20]. The voltage applied to the test body determines the electric field inside the void of given size. The production of an initiatory electron is a stochastic phenomenon, of which the chance would increase with the size of the void sample and exposure rate to the sample. PD inception is determined by random number sampling. We simulated PD inceptions following the scheme and using MATLAB.

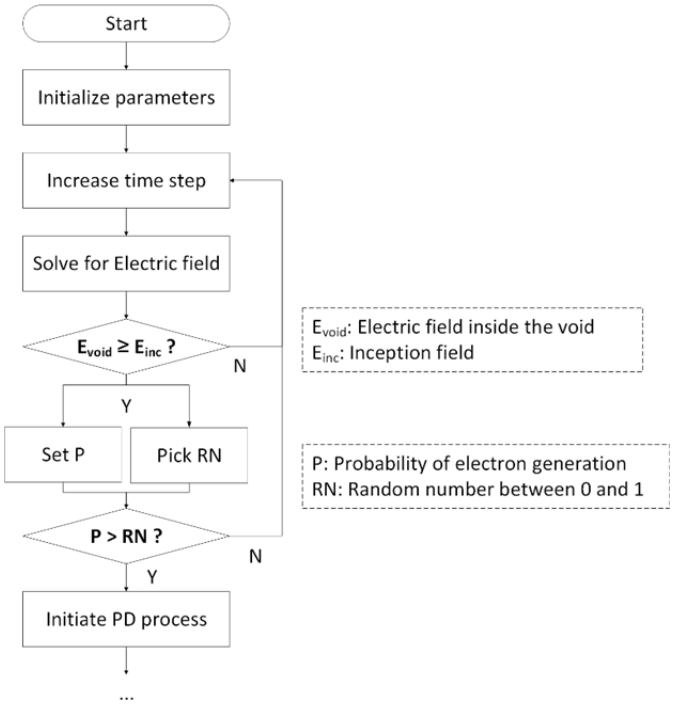

Figure 8. Scheme for judging PD inception in a void sample.

The statistical time lag means the time lapse until PD occurrence after the inception field is reached [20,21]. By

definition, the inception delay is the statistical time lag for the first PD in a void. The inception delay can be as long as several minutes, but the statistical time lag becomes much shorter after the first PD because the previous discharge activities accumulate space charges inside the void that could supply initiatory electrons for the upcoming avalanches [4,5].

The variation in statistical time lag is reflected in the discharge characteristics, including the number of PD signals and average PD pulse height, and the statistical variation of PRPD pattern. We redrew the observations reported by Fruth and Niemeyer [19] in Figure 9, which depicts two distinctive cycle-to-cycle behaviors derived from the simulations. Figure 9 presents the average pulse height of PD signals varying with the electric field inside the void by assuming (a) 100% and (b) 0.1% of initiatory electron generations for each stochastic process. In Figure 9a, PD occurs immediately after the void field reaches the inception field. Hence, the statistical time lag

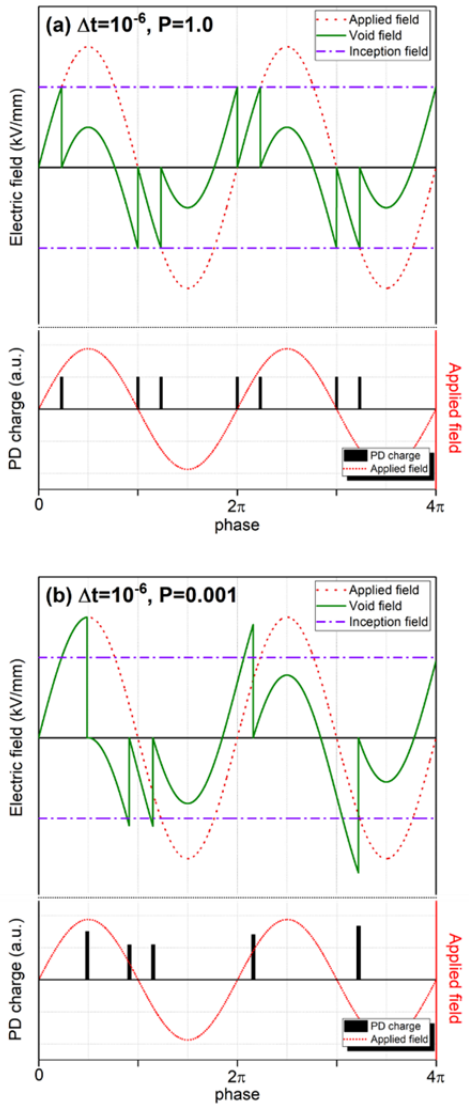

Figure 9. Two distinctive examples of cycle-to-cycle PD behavior and the corresponding PD signals for the initiatory electron generation probability of (a) 1 and (b) 0.001. The PD pulse height is proportional to the respective field collapse; hence, it tends to increase with the statistical time lag.

becomes minimal. More PDs of common charge regularly occur at an earlier phase of each switch of AC cycle. Conversely, the statistical time lag frequently delays the immediate PD occurrence in Figure 9b. Hence, the number of PD signals decreases and both charge and phase angle appear in a random and scattered pattern.

Figure 10 presents the simulated PRPD pattern in comparison with the corresponding experimental data at X-ray exposure rates varying from 2.5 mR/s, 20 mR/s, to 294 mR/s. The experimental patterns were obtained for the minimum applied voltages at which the discharge was sustained under varying exposure rates. Thus, the voltage amplitude inside the void and the inception voltage were set the same for the simulation. The comparable patterns from simulations to those obtained from experiments imply that the simplified model, where increasing X-ray exposure rates were modeled as increasing probabilities of initiatory electron generation, represents appropriately the actual phenomenon. The statistical variation in PRPD pattern is attributed most probably to the change in statistical time lag.

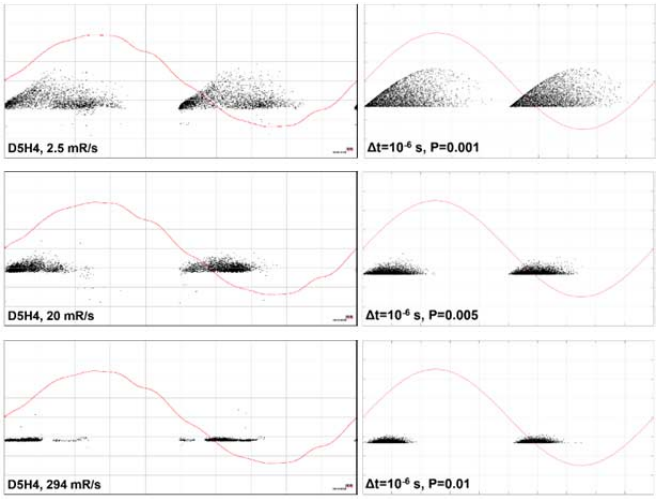

Figure 10. PRPD patterns of experimental (left) and simulation (right) results: lower exposure rate (upper) to higher exposure rate (lower).

4.2 VARIATION OF EXPOSURE RATE IN VOIDS

Given a setup of PD test in our experiments, X-ray exposure rate delivered to a void sample would vary depending on the location of the void in a sizable insulating part such as GIS spacers. The farther the void resides from the entrance of X-ray beam into the insulating body, the further the beam intensity entering the void would be reduced. The reduction in X-ray beam intensity is equivalent to the decrease in exposure rate delivered to the void.

We assessed the attenuation of X-ray beam during the transport in the epoxy-alumina body until reaching the void. Monte Carlo simulation was performed using the MCNP6 code (Monte Carlo N-Particle 6, Los Alamos National Laboratory, USA) for the X-ray beam generated at different tube voltages operable in the HardX-SNU facility. Exposure rate was calculated for a spherical void of the same volume as

void sample D1H1. The void was located at 0-110 mm from the X-ray beam entrance into the epoxy-alumina of 2.31 g/cm^3, which was positioned 5 cm below the X-ray beam exit.

As shown in Figure 11, the exposure rate of the void was reduced with an increasing depth of void location in the insulation epoxy-alumina body in the beam direction. Suppose an extreme case where the thickness of the GIS spacer is 110 mm and a void defect equivalent to sample D1H1 is located at the innermost area. The external voltage should exceed 275 kV to achieve the applied field at a level over the threshold (2.5 kV/mm in Figure 5). X-ray exposure of 0.5 mR/s and over in the void defect is required to eliminate the delay of PD inception. If the minimum detection level is 3000 PDs/min, the X-ray exposure rate should be over 4 mR/s (Figure 6). With X-ray beam generated at 150 kVp, the exposure of the void center at 4 mR/s is accompanied with the exposure of 666.7 mR/s for a void at the outermost surface. With X-ray beam generated at 450 kVp, the corresponding exposure of a void at the surface is 92.5 mR/s, which is in the range confirmed applicable in this study.

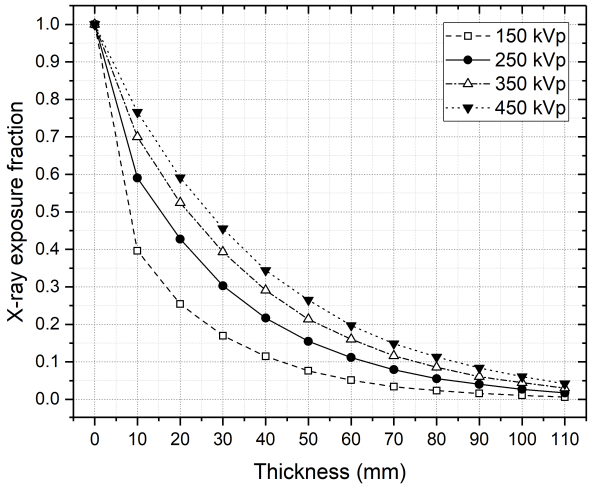

Figure 11. Attenuated X-ray exposure fractions due to material thickness.

5 CONCLUSION

This study regards the method of detecting void defects, as small as 2 mm in diameter of equivalent spherical volume, in the insulating body in a limited, as short as 1 min, time span. Continuous X-ray exposure pursues shortening detection time by generating abundant initiatory electrons to avoid PD inception delay. In consideration that the exposure rate delivered to a void can vary depending on the location of that void, an optimization of the XIPD system will require a range of X-ray exposure rates that effectively initiates PD instead of a single exposure rate. Our observations indicate that PD can be induced without inception delays when the void defect is exposed to X-rays at rates between 0.5 and 294 mR/s even if the void is as small as 1.63 mm in diameter of equivalent spherical volume. High exposure rates up to 294 mR/s do not inhibit PD inceptions but reduce PD pulse heights. Practical setups regarding X-ray beam intensity and the external applied voltage should be determined in specific to the insulating materials to generate sufficient exposure rate to the innermost area.

ACKNOWLEDGMENT

This work has been supported by Power & Industrial Systems R&D Center, HYOSUNG Corporation.

REFERENCES

[1] U. Schichler, W. Koltunowicz, F. Endo, K. Feser, A. Giboulet, A. Girodet, H. Hama, B. Hampton, H. G. Kranz, J. Lopez-Roldan, L. Lundgaard, "Risk assessment on defects in GIS based on PD diagnostics," IEEE Trans. Dielectr. Electr. Insul., vol. 20, no. 6, pp. 2165–2172, Dec. 2013.

[2] G. C. Stone, "Partial discharge diagnostics and electrical equipment insulation condition assessment," IEEE Trans. Dielectr. Electr. Insul., vol. 12, no. 5, pp. 891–903, Oct. 2005.

[3] S. A. Boggs, "Partial discharge – part III: cavity-induced PD in solid dielectrics," IEEE Electr. Insul. Mag., vol. 6, no. 6, pp. 11–20, Nov/Dec. 1990.

[4] L. Niemeyer, "A generalized approach to partial discharge modeling," IEEE Trans. Dielectr. Electr. Insul., vol. 2, no. 4, pp. 510–528, Aug. 1995.

[5] F. Gutfleisch, and L. Niemeyer, "Measurement and simulation of PD in epoxy voids," IEEE Trans. Dielectr. Electr. Insul., vol. 2, no. 5, pp. 729–743, Oct. 1995.

[6] D. Tehlar, U. Riechert, G. Behrmann, M. Schraudolph, L. G. Herrmann, and S. Pancheshnyi, "Pulsed X-ray induced partial discharge diagnostics for routine testing of solid GIS insulators," IEEE Trans. Dielectr. Electr. Insul., vol. 20, no. 6, pp. 2173–2178, Dec. 2013.

[7] A. Cavallini, F. Ciani, G. Mazzanti, and G. C. Montanari, "First electron availability and partial discharge generation in insulation cavities: effect of light irradiation," IEEE Trans. Dielectr. Electr. Insul., vol. 12, no. 2, pp. 387–394, Apr. 2005.

[8] K. Hencken, T. Kaufmann, S. Pancheshnyi, L. Herrmann, and U. Riechert, "Simulation of start electron distribution for insulation material testing using PXIPD," IEEE Trans. Dielectr. Electr. Insul., vol. 23, no. 3, pp. 1636–1642, Jun. 2016.

[9] S. Rizzetto, G. C. Stone, and S. A. Boggs, "The influence of X-rays on partial discharges in voids," in Conference on Electrical Insulation & Dielectric Phenomena - Annual Report 1987, pp. 89–94.

[10] S. Rizzetto, N. Fujimoto, and G. C. Stone, "A system for the detection and location of partial discharges using X-rays," in Conference Record of the 1988 IEEE International Symposium on Electrical Insulation, 1988, pp. 262–266.

[11] J. M. Braun, S. Rizzetto, N. Fujimoto, G. L. Ford, T. Molony, and J. P. Meehan, "X-ray induced partial discharge testing of full-size EHV insulators," in Proceedings of 1996 Transmission and Distribution Conference and Exposition, 1996, pp. 197–203.

[12] N. Fujimoto, S. Rizzetto, and J. M. Braun, "Partial discharge – part XV: improved PD testing of solid dielectrics using X-ray induced discharge initiation," IEEE Electr. Insul. Mag., vol. 8, no. 6, pp. 33–41, Nov/Dec. 1992.

[13] J. M. Braun, S. Rizzetto, N. Fujimoto, and G. L. Ford, "Modulation of partial discharge activity in GIS insulators by X-ray irradiation," IEEE Trans. Dielectr. Electr. Insul., vol. 26, no. 3, pp. 460–468, Jun. 1991.

[14] S. Adili, and C. M. Franck, "Application of pulsed X-ray induced partial discharge measurements," IEEE Trans. Dielectr. Electr. Insul., vol. 19, no. 5, pp. 1833–1839, Oct. 2012.

[15] S. Adili, L. G. Herrmann, and C. M. Franck, "Investigating the inception mechanism of pulsed X-ray triggered partial discharges by time resolved measurements," IEEE Trans. Dielectr. Electr. Insul., vol. 20, no. 5, pp.1780–1788, Oct. 2013.

[16] S. Adili, and C. M. Franck, "Partial discharges characterization in spherical voids using ultra-short X-ray pulses," IEEE Trans. Dielectr. Electr. Insul., vol. 21, no. 2, pp. 791–799, Apr. 2014.

[17] K. M. Lee, S. R. Kim, and E. H. Kim, "Characterization of dose delivery in a hard X-ray irradiation facility," J. Nucl. Sci. Technol., vol. 49, no. 6, pp. 655–661, Jun. 2012.

[18] S. Devic, N. Tomic, and D. Lewis, "Reference radiochromic film dosimetry: review of technical aspects," Phys. Medica, vol. 32, pp. 541–556, Mar. 2016.

[19] B. Fruth, and L. Niemeyer, "The importance of statistical characteristics of partial discharge data," IEEE Trans. Dielectr. Electr. Insul., vol. 27, no. 1, pp. 60–69, Feb. 1992.
[20] H. A. Illias, M. A. Tunio, H. Mokhlis, G. Chen, and A. H. A. Bakar, "Determination of partial discharge time lag in void using physical model approach," IEEE Trans. Dielectr. Electr. Insul., vol. 22, no. 1, pp. 463–471, Feb. 2015.
[21] H. Illias, G. Chen, and P. Lewin, "Partial discharge behavior within a spherical cavity in a solid dielectric material as a function of frequency and amplitude of the applied voltage," IEEE Trans. Dielectr. Electr. Insul., vol. 18, no. 2, pp. 432–443, Apr. 2011.

Ji-Yong Shin was born in Seoul, South Korea in 1990. He received the BSc degree in nuclear engineering from Seoul National University, Seoul, South Korea in 2015. He has been a PhD student since March 2015 in the same university. His research interests include industrial applications of radiation, radiation protection, and radiation transport modeling.

Eun-Hee Kim was born in Seoul, South Korea, in 1964. She received the BSc degree from Seoul National University, Seoul, South Korea, in 1986, the MSc degree from Seoul National University, Seoul, South Korea, in 1988 and the PhD degree from Texas A&M University, Texas, USA, in 1995. She has been an associate professor in Department of Nuclear Engineering at Seoul National University since 2006. Her research interests include theoretical and experimental analyses of physical and biological aspects in radiation effects on human body for radiation protection purposes, radiation therapy planning, radiation system design for basic studies, and irradiation prescription for industrial applications.

Sung-wook Kim was born in Busan, Korea in 1981. He received the BSc degree from Korea Maritime and Ocean University, Busan, South Korea, in 2008, the MSc degree from Korea Maritime and Ocean University, Busan, South Korea in 2010 and the PhD degree from Korea Maritime and Ocean University, Busan, South Korea in 2017. Since 2010, he has worked for R & D center of Hyosung corporation and is one of the members in charge of partial discharge and dissolved gas analysis project. His research interests are PD and DGA diagnosis method of power equipment. He may be reached at Hyosung corporation, 454-2, Nae-Dong, Changwon-City, Gyeongsangnam-Do, Korea or at number1@hyosung.com.

Hyang-eun Jo was born in Tongyoung, Korea in 1987. She received the BSc degree from Korea Maritime and Ocean University, Busan, South Korea, in 2010, the MSc degree from Korea Maritime and Ocean University, Busan, South Korea in 2012 and the PhD degree from Korea Maritime and Ocean University, Busan, South Korea in 2016. Since then, she has worked for R & D center of Hyosung corporation. Her research interests are partial discharge of GIS and dissolved gas analysis diagnosis method of power transformers. She may be reached at Hyosung corporation, 454-2, Nae-Dong, Changwon-City, Gyeongsangnam-Do, Korea or at hejo@hyosung.com.

Jae-ryong Jung was born in Busan, South of Korea in 1976. He received the B.Sc. in 1999, M.Sc. in 2001 from the Busan National University, Busan, south of Korea. Since then, he has worked for R & D center of Hyosung corporation and is a chief researcher. His research interests are partial discharge diagnostics system for power apparatus and asset management solution for substation. He is a Korea representitive member of CIGRE SC B3. He may be reached at Hyosung corporation, 171, Yeodeok-ro, Changwon-City, Gyeongsangnam-Do, Korea or at jrjung@hyosung.com.